15/10/2018

# A First Time in Human, Microdose, Positron Emission Tomography Study of the Safety, Immunogenicity, Biodistribution and Radiation Dosimetry of [$^{18}$F]FB-A20FMDV2 for Imaging the Integrin αvβ6

Nicholas Keat[1], Julia Kenny[2], Keguan Chen[3], Mayca Onega[1], Nadia Garman[4], Robert J Slack[5], Christine A Parker[6], R Thomas Lumbers[5]†, Will Hallett[1], Azeem Saleem [1], Jan Passchier[1], Pauline T Lukey[5]

1. Imanova Ltd, London UK
2. *In vitro In vivo* Translation, GlaxoSmithKline R&D, Ware UK
3. Immunogenicity and clinical immunology, GlaxoSmithKline R&D, Upper Merion, USA
4. Clinical operations, GlaxoSmithKline R&D, Stevenage, UK
5. Fibrosis Discovery Performance Unit, GlaxoSmithKline R&D, Stevenage, UK
6. Clinical imaging, GlaxoSmithKline R&D, Stevenage, UK

† Present address: Institute of Cardiovascular Science, Faculty of Population Health, University College London, London WC1E 6BT, U.K.

**Corresponding author**

Pauline T. Lukey
Fibrosis Discovery Performance Unit
GlaxoSmithKline R&D
Stevenage, UK
Pauline.t.lukey@gsk.com

15/10/2018


# Abstract

**Background**

The αvβ6 integrin is involved in the pathogenesis of cancer and fibrosis. Levels of αvβ6 expression measured by immunohistochemistry have been shown to provide clinically relevant prognostic and potentially theranostic information. A radio-labelled 20-amino acid αvβ6-binding peptide, derived from the foot and mouth virus (A20FMDV2), has been developed to image αvβ6 levels pre-clinically.

**Aim**

To translate pre-clinical findings into a clinical PET imaging protocol to measure the expression of αvβ6 in humans.

**Methods**

A first time in human study was conducted in healthy subjects to measure the safety, tolerability, immunogenicity, biodistribution and radiation dosimetry of [$^{18}$F]FB-A20FMDV2. Prior to the clinical study, pre-clinical toxicology was undertaken using FB-A20FMDV2 and a direct immunoassay was developed and validated to detect antibodies to A20FMDV2. Four healthy subjects (two males and two females) were enrolled in the study and received a single microdose of [$^{18}$F]FB-A20FMDV2. Subjects underwent a multibed positron emission tomography (PET) scan of the whole body (vertex to mid-thigh) over 3+ hours.

**Results**

There were no findings in the pre-clinical toxicology assessments of FB-A20FMDV2. The PET ligand was well tolerated in humans with no peptide-related clinically significant adverse events. No anti-A20FMDV2 antibodies were detected before or after dosing with the PET ligand. On visual inspection of PET images, uptake of radioactivity was observed in the thyroid, salivary glands, liver, stomach wall, spleen, ureters and bladder. Time-activity curves from the regions of interest indicated that the highest activity was observed in the bladder content, followed by the kidneys, small intestine, stomach, liver, spleen, thyroid and gallbladder. The largest component of the residence times was the voided urine, followed by muscle, bladder and liver. Using the mean residence time over all subjects as input to Organ Level INternal Dosimetry Assessment/EXponential Modelling software (OLINDA/EXM), the effective dose was determined to be 0.0217 mSv/MBq; using residence times from single subjects gave a standard deviation of 0.0020 mSv/MBq from the mean. The critical organ was the urinary bladder, with an absorbed dose of 0.18 mGy/MBq.

**Conclusion**

[$^{18}$F]FB-A20FMDV2 caused no adverse effects in healthy subjects and has an effective dose that enables multiple scans in a single subject.

# Introduction

The αvβ6 integrin is a cell surface adhesion receptor that, in its activated form, interacts with extra-cellular ligands bearing the Arginine-Glycine-Aspartic Acid (RGD) tri-peptide sequence (Munger et al. 1999). It plays a role in the aetiology and progression of a number of pathological conditions including cancer and fibrosis and as such it is an important prognostic biomarker as well as a potential drug target.

Key ligands for αvβ6 include the latency associated peptides (LAPs) of transforming growth factor beta1 and beta3 (LAPβ1 & LAPβ3) as well as extra-cellular matrix (ECM) ligands such as fibronectin, tenascin and vitronectin (Busk, Pytela, and Sheppard 1992; Prieto, Edelman, and Crossin 1993). Binding of ECM ligands to the integrin receptor can promote cell adhesion, activation of intra-cellular signalling pathways and local release of activated TGFβ from latent complexes in the matrix (Munger et al. 1999; Annes, Rifkin, and Munger 2002; Henderson and Sheppard 2013). αvβ6 is up-regulated on many cancers, including pancreatic, breast, ovarian, colon, and over 90% of oral squamous cell carcinoma (Thomas et al. 2001; Breuss et al. 1995). Furthermore, expression of αvβ6 correlates with development of metastasis in gastric cancer (Kawashima et al. 2003), is linked with a dramatic reduction in survival from colon cancer (Bates et al. 2005), and is reported to promote both the survival and invasive potential of carcinoma cells (Thomas, Nystrom, and Marshall 2006; Thomas et al. 2002; Nystrom et al. 2006; Janes and Watt 2006). αvβ6-mediated activation of TGFβ promotes myofibroblast differentiation, proliferation and collagen synthesis as part of normal physiological wound healing (Roberts, Sporn, and Assoian 1986; Roberts and Sporn 1989). However, when this process persists and fails to resolve, the result is a pathological elaboration of ECM which results in irreversible organ scarring, ultimately resulting in organ failure and death (Thomas et al. 2016).

The foot and mouth disease virus (FMDV) uses αvβ6 to access the intracellular environment of the host and thus causes the symptoms of foot and mouth disease. In fact, the envelope protein of the virus contains a 20–amino acid peptide sequence, NAVPNLRGDLQVLAQKVART (A20FMDV2) that

mediates FMDV infection by binding to αvβ6 (Jackson et al. 2000; Monaghan et al. 2005; Burman et al. 2006). Phage display analysis identified the DLXXL sequence as a key moiety responsible for αvβ6 specificity while having only minimal interactions with other RGD-integrins (e.g αvβ3, αvβ5, and aIIbβ3) (Kraft et al. 1999). The high affinity and selectivity (Slack et al. 2016) as well as the automated and GMP compatible radiochemistry and pre-clinical radiodosimetry (Onega 2017) of this A20FMDV2 peptide for αvβ6 have recently been described.

In this manuscript, we describe the safety, tolerability, immunogenicity, biodistribution and radiation dosimetry of [$^{18}$F]FB-A20FMDV2 (also known as [$^{18}$F]IMAFIB, GSK2634673) in preparation of its use as a PET ligand for the delineation of αvβ6 in humans. If successful, this PET ligand may be useful in the clinical management of patients with cancer or fibrosis, since levels of expression of αvβ6 may be of prognostic value (Saini et al. 2015; Hussain et al. 2014) and potentially could be used to make treatment decisions in clinical practice. In addition, it may prove to be valuable during development of new therapies that target αvβ6, as an *in vivo* imaging tool for demonstrating target engagement. Prior to conducting this first time in human study with [$^{18}$F]FB-A20FMDV2, various potential risks were identified and strategies to manage these risks were developed. Pre-clinical toxicology was conducted to support microdosing in humans (up to a maximum mass dose of 100µg, as detailed in the International Committee on Harmonization (ICH) M3 R2). Potential for immunogenic risk was explored through development of an immunogenicity assay to monitor pre-existing as well as induced antibodies as a result of exposure to this FMDV2 peptide within this study.

# Methods

## Study conduct

Subjects were screened and recruited at Hammersmith Medicines Research (HMR), London, UK and imaging assessments were conducted at the Imanova Centre for Imaging Sciences, London, UK. The study was approved by the London – Brent Research Ethics Committee, UK (reference 13/LO/1792), and permission to administer radioisotopes was obtained from the Administration of Radioactive

Substances Advisory Committee (ARSAC) of the UK (Ref: 630/3925/30809). The PETAL (**PET** study of **α**vβ6 in **l**ungs) study is recorded in clinical trials.gov as 'A Validation and Dosimetry Study of GSK2634673F PET Ligand' (NCT02052297; RES116235) and the dosimetry data presented here forms part of that study.

## Subjects

Four healthy human subjects (two male, two female, ages 48-65) were enrolled in the study after providing written informed consent. The main inclusion criteria were male or female subjects aged 45 years or older and free from any clinically significant illness or disease. The main exclusion criteria included prior radiation exposure to greater than 10 mSv over the past 3 years or greater than 10 mSv in a single year including the proposed study; previous or current exposure to animals that may harbour the foot and mouth disease virus (FMDV2); and previous long term (>= 3 months) residence in a country where FMDV2 is endemic (such as certain areas of Africa, Asia and South America).

## Pre-clinical Toxicology

FB-A20FMDV2 (a non-radioactive homologue of the proposed PET labelled peptide) was screened against a broad range of *in vitro* pharmacological targets (receptors, ion channels, enzymes and transporters) that were distinct from the intended therapeutic target (αvβ6 integrin receptor) to assess the potential for off-target interactions.

A limited number of nonclinical toxicity studies were performed to evaluate the potential toxicity of the triacetate salt of FB-A20FMDV2, based on the principles of the ICH M3(R2) guideline [ICH 2009] to support the human microdose PET study. The haemolytic potential of FB-A20FMDV2 solutions in 0.9% w/v aqueous sodium chloride (Fresenius Kabi, Bordon, UK) at concentrations of 0.04 and 0.4 mg/mL were assessed *in vitro* in rat and human blood. These concentrations were selected to match the concentrations used in a subsequent rat toxicity study. The rat was selected as a relevant species as they are known to express αvβ6 integrin receptors (Onega 2017; Popov et al. 2008). In order to examine the toxicity and irritancy potential, groups of 10 male and 10 female Crl:WI (Han) rats (9 to

11 week of age) received  a single intravenous dose of vehicle (0.9% w/v aqueous sodium chloride) or FB-A20FMDV2 at 0.2 mg/kg or 2 mg/kg, at a dose volume of 5mL/kg. These doses provided approximately 100-fold and 1000-fold the maximum permissible human microdose on a mg/kg basis. Animals in this cohort were sacrificed 24 hours after dosing.  Additional groups of 5 male and 5 female rats were treated similarly and then remained off-dose for a 14-day period to investigate the regression/progression of any target organ toxicity present at the end of the treatment period or delayed onset of any target organ toxicity. All animal studies were ethically reviewed and carried out in accordance with the Animals (Scientific Procedures) Act 1986 and the GSK Policy on the Care, Welfare and Treatment of Laboratory Animals.

## Immunogenicity Assay

A direct immunoassay was developed and validated using a pool of A20FMDV2 (GSK3225458) peptide labelled with biotin either at the N- or C- terminus to capture antibodies to the peptide. Captured antibodies were detected using a horseradish peroxidise (HRP) conjugated polyclonal goat anti-human IgG H+L reagent capable of binding to human antibodies regardless of isotype (Supplementary

). Negative control (NC) was prepared from pooled normal human serum and was used to define sensitivity and to normalize results. Screening and confirmation cut points were determined during method validation.

Serum samples for immunogenicity screening were obtained from all four subjects prior to administration of [$^{18}$F]FB-A20FMDV2 and at follow up (2 – 4 weeks after administration of [$^{18}$F]FB-A20FMDV2. Samples were stored at -70°C until assayed. More details are available in the supplementary information

## Imaging

Healthy human subjects were imaged for up to 3.5 hours on a Siemens Biograph 6 TruePoint PET-CT scanner (Siemens Healthcare, Erlangen, Germany) following intravenous administration of [$^{18}$F]FB-A20FMDV2, prepared according to (Onega 2017).

Prior to injection, each subject received a CT scan for attenuation correction (AC) over 6 to 7 PET bed lengths covering a range from vertex of head to mid-thigh using 130 kV tube potential, and 15 effective mAs exposure with 0.6 second gantry rotation time and spiral pitch of 1.5. CT image data was acquired with 6x3 mm channels, and reconstructed to 5 mm slices at 3 mm intervals and 700 mm field of view.

For each subject, PET scanning was initiated at the time of injection, and a series of 6 whole body scans was performed. Each scan consisted of 6-7 bed positions (depending on subject size), with the duration increasing for subsequent scans, through 1, 2, 5, 5, 7 and 7 minutes per bed position. Between whole body scans 4 and 5, the subject was removed from the scanner bed to void their bladder and move around for around 20 minutes to limit discomfort. After this break, a second AC CT was performed before PET imaging was resumed. PET images were reconstructed on a 256x256 matrix, with a zoom of 1.3 m using ordered subsets with expectation maximisation (OSEM) algorithm employing 3 iterations and 21 subsets and a 5 mm Gaussian image filter. Corrections for scatter, attenuation and decay (to the start of each scan) were applied.

## Image Analysis

Image analysis was performed on a Siemens Inveon Research Workplace (IRW; Siemens Healthcare, Erlangen, Germany) workstation, version 4.0.1.14. Regions of Interest (ROIs) were drawn on the PET-CT datasets, delineating as many organs that are relevant to dosimetry as possible, in particular those that are defined by OLINDA/EXM, version 1.1 (Organ Level INternal Dosimetry Assessment/EXponential Modelling software) (Stabin, Sparks, and Crowe 2005) as source organs. CT anatomy and/or PET uptake was used as a guide, with one set of ROIs being drawn for the first four

scans, and another drawn after the bladder void and rest prior to scans 5 and 6. A separate bladder ROI was used for each frame, which took into account the change in size as the bladder filled and emptied over the course of the study. The activity concentrations in these ROIs were exported from IRW, and imported to Microsoft Excel (Microsoft, Redmond, Washington, US) for further analysis. Organ ROI activity concentrations were tabulated for each frame, to create time activity curves (TAC) which were integrated, with the activity in each organ at the end of the sixth scan being assumed to decay in situ without further redistribution. These values were then multiplied by the organ volume in the Cristy and Eckerman adult phantom according to (Stabin and Siegel 2003) to calculate the organ residence time (this is the equivalent duration in hours that a single MBq of activity is present in that organ per injected MBq of radioligand, units of MBq.h/MBq).

The bladder was treated separately, with the total activity in the bladder in each frame being input to a model employing an exponential fill and void, fitting parameters for the exponential rate and magnitude as well as the void time and voided fraction. This model was then used with a 2 hour voiding period being fitted to the measured data, and integrated to calculate the bladder residence time.

The mean organ residence times over all subjects were used as the input to OLINDA/EXM, which calculated the absorbed dose to each of the relevant target organs (units mGy/MBq), and provided the resulting effective dose per unit injected activity (units mSv/MBq).

To provide a measure of the variability of this result, the effective dose per unit injected activity was also calculated using the residence times from each individual subject.

# Results

## Pre-clinical Toxicology

FB-A20FMDV2 did not demonstrate any off- target activity when screened against a broad range of *in vitro* pharmacological targets (receptors, ion channels, enzymes and transporters), including a

cardiovascular liability panel. Since FB-A20FMDV2 is a large molecular weight peptide, access to the ion channels was limited and it was considered unlikely the peptide would affect the hERG channel. Therefore, taken together, further nonclinical safety pharmacological assessment was not considered necessary.

The haemolytic potential of FB-A20FMDV2 in 0.9% w/v aqueous sodium chloride at concentrations of 0.04 and 0.4 mg/mL was assessed *in vitro* in rat and human blood. As anticipated, no evidence of haemolysis was observed at either concentration tested, and therefore, this formulation was deemed suitable for intravenous use. Local irritancy and target organ toxicity was investigated in an intravenous extended single dose toxicity study in rats at 0.2 or 2 mg/kg with a 14 day off-dose period. Both doses were well tolerated and no treatment-related clinical signs of toxicity, changes in body weight gain or food consumption were observed. In addition, no treatment related changes in clinical pathology parameters (haematology, clinical chemistry and coagulation) were observed at either dose. At both terminal necropsy and following the 14 day off-dose period, there were no FB-A20FMDV2 -related macroscopic or microscopic observations. Stage-dependent qualitative evaluation of spermatogenesis in the testes was performed on all male rats given vehicle and 2 mg/kg FB-A20FMDV2. The testes revealed normal progression of the spermatogenic cycle and the expected cell associations and proportions in the various stages of spermatogenesis were present.

Thus FB-A20FMDV2 was shown to be non-toxic and supports microdosing in humans up to 100 μg [$^{18}$F]FB-A20FMDV2 (equivalent to 2 μg/kg for a 50 kg individual), with anticipated cover (at the human dose) of 1000-fold on a mg/kg basis.

## Clinical Safety and tolerability

The PET scans were well-tolerated and all four subjects completed the scans as planned. None of the 4 subjects imaged had any [$^{18}$F]FB-A20FMDV2 or PET procedure associated adverse events. Three AEs were reported in this study comprising abdominal cramps, erythema of conjunctiva and

heaviness of arms. In the opinion of the investigator none of these was due to the radioligand or the imaging procedure.

## Immunogenicity

The screening and confirmation cut points were statistically established during validation and were 2.10 relative O.D. (ROD) and 48.4% inhibition, respectively. To differentiate peptide-boosted true positive from the pre-existing positive responses in healthy subject population, a ratio of post-dose ROD over pre-dose ROD was calculated. Samples with a ratio of ≥2 were reported as peptide-boosted positives. Based on clinical sample testing results, all four human subjects were negative in the anti-peptide antibody assays. Details of the assay validation are available in the supplementary information.

## PET imaging

**Four subjects were scanned, with demographic and radioligand administration details given in Table 1. Subject demographic and scan details**

| Subject | Gender | Age (years) | Weight (kg) | Scan duration (minutes) | Injected activity (MBq) | Specific activity (GBq/μmol) | Injected mass (μg) |
|---|---|---|---|---|---|---|---|
| 1 | M | 47 | 95.0 | 204 | 145 | 25.5 | 13.0 |
| 2 | M | 58 | 75.6 | 214 | 121 | 26.4 | 10.5 |
| 3 | F | 59 | 85.6 | 213 | 134 | 35.2 | 8.7 |
| 4 | F | 64 | 75.6 | 184 | 98 | 84.3 | 2.7 |

`

. PET images through a single coronal slice presented in Figure 1 show the activity uptake and clearance by tissue organs over the 3+ hour total study time for subject 1. Organs that are clearly visible in this slice through the body include the thyroid, salivary glands, liver, stomach wall, spleen, ureters and bladder. Figure 2 shows coronal and sagittal CT views through subject 1, overlaid with organ ROIs.

Time-activity curves (TACs) from the ROIs through the 13 most active organs are shown in Figure 3 (colours of organ ROIs and TACs are matched. TACs with max value < 2 kBq/mL are not shown and include: muscle, testes, cortical bone, trabecular bone, bone marrow, lungs and brain). Greatest activity concentration was observed for bladder content which, in contrast to the other organs, increases after the first scan, with the interruption of the void at 2 hours. The other notable organs of uptake include the kidneys, small intestine, stomach wall, liver, spleen, thyroid and gallbladder, whose TACs generally have their highest point in scan 1, and decrease broadly linearly over this logarithmic graph, indicating exponential clearance. TACs for all four subjects were broadly similar.

Organ residence times for OLINDA source organs that could be identified from scan images, for each subject, as well as the mean across all subjects, are shown in Table 1. Residence times for breast tissue were assessed for female subjects only, and testes for males only. 'Organ total' is the sum of the residence times measured in individual organ ROIs. 'Voided urine' is calculated from the quantity of urine voided according to the modelled bladder fit. The total residence times for all organs for an injected radioligand should add up to the mean lifetime for that isotope, which for fluorine-18 is 2.64 hours. The 'Remainder' residence time is therefore the activity injected which was not measured within ROIs in the image, and is given by the mean lifetime minus the organ total and voided urine.

The largest component of the mean residence time is the voided urine, followed by remainder, muscle, bladder and liver. The residence time is affected not only by the activity concentration but also the organ mass, hence the influence of larger organs like muscle and liver.

The mean residence times were entered into OLINDA/EXM, and the results are shown in Table 2, showing the organ beta, gamma and total absorbed doses (mGy) and effective dose contribution (mSv) from each organ, as well as the total effective dose per injected MBq. The beta dose to the stomach wall was adjusted to correct for OLINDA/EXM's use of the stomach contents as a source organ, rather than the wall itself.

The critical organ is the urinary bladder, with an absorbed dose of 0.198 mGy/MBq. The effective dose derived from the mean of the organ residence times was 0.0217 mSv/MBq. The effective dose derived by using each individual subject's residence times range from 0.0217 to 0.0247 mSv/MBq, resulting in a standard deviation of 0.0020 mSv/MBq.

## Discussion

This study describes the first-in-human administration of [$^{18}$F]FB-A20FMDV2 a PET ligand that has been shown pre-clinically to bind with high affinity and specificity to the integrin αvβ6 (Hausner et al. 2007; Hausner et al. 2009; John et al. 2013; Slack et al. 2016; Onega 2017). αvβ6 is involved in the aetiology and pathogenesis of cancer and fibrosis and its expression levels have prognostic and theranostic implications for patient management and drug development. Thus, a PET ligand that can be used to non-invasively measure expression levels of this integrin in humans is likely to have broad clinical application in both patient management and the development of new treatments that target αvβ6. The current study provides information about the safety, tolerability and biodistribution of [$^{18}$F]FB-A20FMDV2 in healthy subjects, as well as the radiation dosimetry of this ligand.

The observed benign profile in the four humans tested in this study supports the lack of findings in the pre-clinical toxicology. In addition, no antibodies to the ligand were detected either before or after administration of the ligand.

Immunohistochemistry in various mouse organs, using a monoclonal antibody specific for αvβ6, revealed that this integrin is expressed constitutively at high or moderate levels in the epithelium of the gall bladder, stomach, duodenum, ileum and colon (Saha et al. 2010). Low levels of αvβ6 expression were detected in the mouse skin (Saha et al. 2010). These data were supported by SPECT imaging data using indium-labelled A20FMDV2 but the lung was added to the list of organs expressing αvβ6 (Saha et al. 2010). PET images from the current human study show focal uptake in the small intestine, stomach, liver, spleen, thyroid and gallbladder, but the majority of the activity

was cleared to the bladder by the kidneys. The largest organ doses were found within the abdominal cavity, with the highest value to the bladder wall, then the kidneys, liver, small intestine, uterus, stomach and spleen.

The effective dose, which is 0.0217 mSv/MBq, is lower than the figure from rat data of 0.0335 mSv/MBq (Onega 2017), largely resulting from the lower residence time in the bladder and small intestine in human, which have longer residence times in rat. The result is fairly typical for a fluorine-18 based ligand, and is close to the value of 0.019 mSv/MBq (Hays et al. 2002) for the most widely used PET ligand, [$^{18}$F]Fludeoxyglucose (FDG). The critical organ is the urinary bladder, which is common for a ligand that is cleared from the body by a renal route.

In conclusion, [$^{18}$F]FB-A20FMDV2 is a safe PET radioligand for future clinical studies to investigate changes in αvβ6 receptor availability as a result of increased expression in disease or following direct competition with a drug candidate. It has the potential to be used as a diagnostic, prognostic and theranostic marker in the clinical management of cancer and fibrosis. In addition, [$^{18}$F]FB-A20FMDV2 may be used in the development of novel therapies that target αvβ6.

**Acknowledgements**

The authors acknowledge staff at Imanova Ltd and GSK R&D Ware, Upper Merrion and Stevenage for their professional conduct and successful delivery of all study procedures. The authors acknowledge the work of Andy Brown in initial aspects of the study setup procedures.

**Disclosures**

This study is sponsored by GlaxoSmithKline R&D (study numbers 200262/NCT02612051). GlaxoSmithKline reviewed the manuscript for factual accuracy.

Nicholas Keat, Mayca Onega, Will Hallett, Azeem Saleem and Jan Passchier are all employees of Imanova, UK Ltd. Julia Kenny, Keguan Chen, Nadia Garman, Robert J Slack, Christine A Parker, Tom

15/10/2018

Lumbers and Pauline T Lukey are employees (or were employees at the time of the study) of GlaxoSmithKline R&D and own shares in the company.

# Tables

**Table 1. Subject demographic and scan details**

| Subject | Gender | Age (years) | Weight (kg) | Scan duration (minutes) | Injected activity (MBq) | Specific activity (GBq/µmol) | Injected mass (µg) |
|---|---|---|---|---|---|---|---|
| 1 | M | 47 | 95.0 | 204 | 145 | 25.5 | 13.0 |
| 2 | M | 58 | 75.6 | 214 | 121 | 26.4 | 10.5 |
| 3 | F | 59 | 85.6 | 213 | 134 | 35.2 | 8.7 |
| 4 | F | 64 | 75.6 | 184 | 98 | 84.3 | 2.7 |

`

**Table 1. Residence times (hours) of [$^{18}$F]FB-A20FMDV2 for each organ (each individual and mean)**

| Residence time (MBq.h/MBq) | Subject 1 | Subject 2 | Subject 3 | Subject 4 | Mean |
|---|---|---|---|---|---|
| Brain | 0.0035 | 0.0037 | 0.0034 | 0.0047 | **0.0038** |
| Breasts | | | 0.0034 | 0.0027 | **0.0030** |
| Gallbladder | 0.0026 | 0.0038 | 0.0036 | 0.0063 | **0.0041** |
| Lower Large Intestine | 0.0072 | 0.0085 | 0.0170 | 0.0053 | **0.0095** |
| Small Intestine | 0.0619 | 0.0681 | 0.0571 | 0.0633 | **0.0626** |
| Stomach | 0.0217 | 0.0208 | 0.0183 | 0.0165 | **0.0193** |
| Upper Large Intestine | 0.0105 | 0.0112 | 0.0117 | 0.0155 | **0.0122** |
| Heart Contents | 0.0093 | 0.0111 | 0.0087 | 0.0112 | **0.0101** |
| Heart Wall | 0.0065 | 0.0077 | 0.0060 | 0.0078 | **0.0070** |
| Kidneys | 0.0760 | 0.0674 | 0.0560 | 0.0983 | **0.0744** |
| Liver | 0.0928 | 0.1796 | 0.1627 | 0.2084 | **0.1609** |
| Lungs | 0.0370 | 0.0326 | 0.0360 | 0.0500 | **0.0389** |
| Muscle | 0.6335 | 0.5868 | 0.3425 | 0.4109 | **0.4934** |
| Red Marrow | 0.0125 | 0.0131 | 0.0098 | 0.0115 | **0.0117** |
| Cortical Bone | 0.0420 | 0.0294 | 0.0251 | 0.0397 | **0.0341** |
| Trabecular Bone | 0.0117 | 0.0273 | 0.0074 | 0.0212 | **0.0169** |
| Spleen | 0.0086 | 0.0183 | 0.0118 | 0.0137 | **0.0131** |
| Testes | 0.0007 | 0.0010 | | | **0.0009** |
| Thyroid | 0.0009 | 0.0007 | 0.0008 | 0.0010 | **0.0008** |
| Urinary Bladder | 0.3410 | 0.3649 | 0.5587 | 0.3680 | **0.4082** |
| Organ total | 1.3801 | 1.4562 | 1.3400 | 1.3559 | **1.3850** |
| Voided urine | 0.5996 | 0.6246 | 1.0001 | 0.6576 | **0.7205** |
| Remainder | 0.6605 | 0.5593 | 0.3001 | 0.6266 | **0.5346** |

**Table 2. Absorbed and effective dose to each organ**

| Target Organ | Beta absorbed dose (mGy/MBq) | Gamma absorbed dose (mGy/MBq) | Total absorbed dose (mGy/MBq) | Effective Dose Contribution (mSv/MBq) |
|---|---|---|---|---|
| Adrenals | 1.01E-03 | 7.62E-03 | 8.63E-03 | 4.31E-05 |
| Brain | 3.73E-04 | 1.41E-03 | 1.79E-03 | 8.93E-06 |
| Breasts | 1.19E-03 | 2.72E-03 | 3.91E-03 | 1.96E-04 |
| Gallbladder Wall | 6.11E-03 | 1.05E-02 | 1.66E-02 | 0.00E+00 |
| LLI Wall | 5.63E-03 | 1.18E-02 | 1.74E-02 | 2.09E-03 |
| Small Intestine | 1.13E-02 | 9.82E-03 | 2.11E-02 | 1.06E-04 |
| Stomach Wall | 1.11E-02 | 7.65E-03 | 1.87E-02 | 2.25E-03 |
| ULI Wall | 4.66E-03 | 9.93E-03 | 1.46E-02 | 7.30E-05 |
| Heart Wall | 4.64E-03 | 5.83E-03 | 1.05E-02 | 0.00E+00 |
| Kidneys | 3.46E-02 | 1.58E-02 | 5.04E-02 | 2.52E-04 |
| Liver | 1.17E-02 | 1.16E-02 | 2.33E-02 | 1.16E-03 |
| Lungs | 5.42E-03 | 5.00E-03 | 1.04E-02 | 1.25E-03 |
| Muscle | 2.46E-03 | 5.51E-03 | 7.96E-03 | 3.98E-05 |
| Ovaries | 1.01E-03 | 1.17E-02 | 1.27E-02 | 2.54E-03 |
| Pancreas | 1.01E-03 | 8.10E-03 | 9.11E-03 | 4.56E-05 |
| Red Marrow | 1.96E-03 | 5.55E-03 | 7.52E-03 | 9.02E-04 |
| Osteogenic Cells | 5.32E-03 | 4.87E-03 | 1.02E-02 | 1.02E-04 |
| Skin | 1.01E-03 | 3.04E-03 | 4.05E-03 | 4.05E-05 |
| Spleen | 9.95E-03 | 8.77E-03 | 1.87E-02 | 9.36E-05 |
| Testes | 3.19E-03 | 7.37E-03 | 1.06E-02 | 0.00E+00 |
| Thymus | 1.01E-03 | 4.20E-03 | 5.21E-03 | 2.61E-05 |
| Thyroid | 5.36E-03 | 4.12E-03 | 9.47E-03 | 4.74E-04 |
| Urinary Bladder Wall | 1.36E-01 | 6.26E-02 | 1.98E-01 | 9.92E-03 |
| Uterus | 1.01E-03 | 1.83E-02 | 1.93E-02 | 9.64E-05 |
| Total Body | 2.86E-03 | 5.48E-03 | 8.33E-03 | 0.00E+00 |
| **Effective Dose (mSv/MBq)** | | | | **2.17E-02** |

# Figures

**Figure 1. PET activity though a single coronal slice for subject 1, over the 6 scans (scale 0-10 kBq/mL, mid scan time points shown in h:mm:ss).**

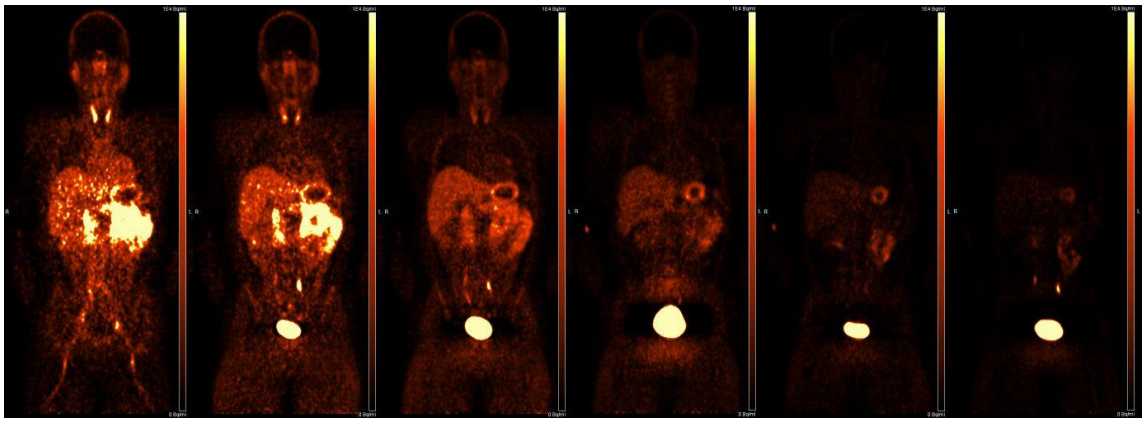

**Figure 2. Organ Regions of Interest (ROIs) for subject 1, organs are coloured to match those in TACs (Figure 3)**

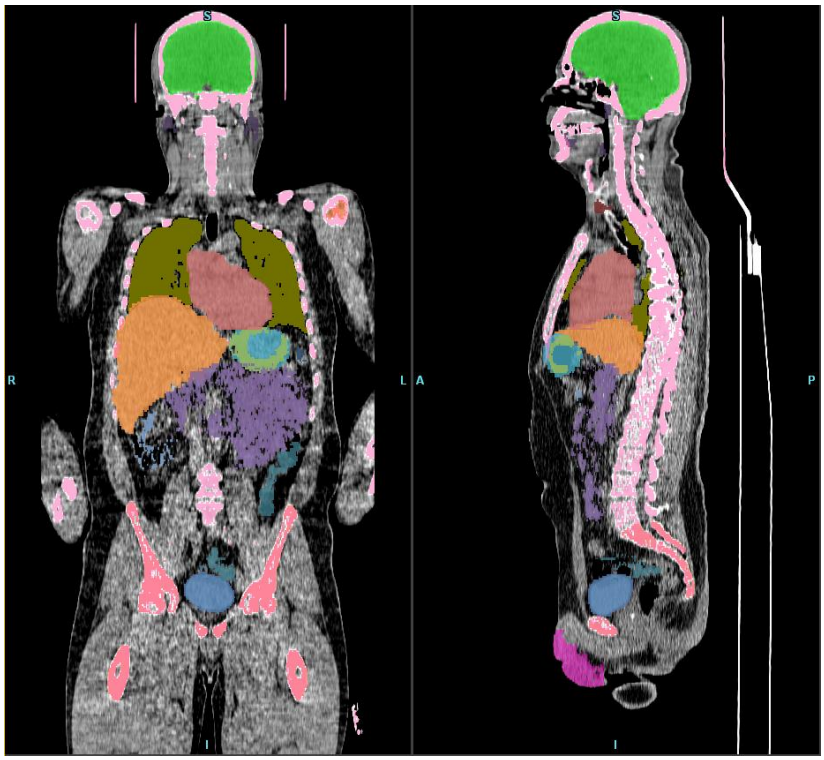

**Figure 3. Organ time-activity curves for subject 1**

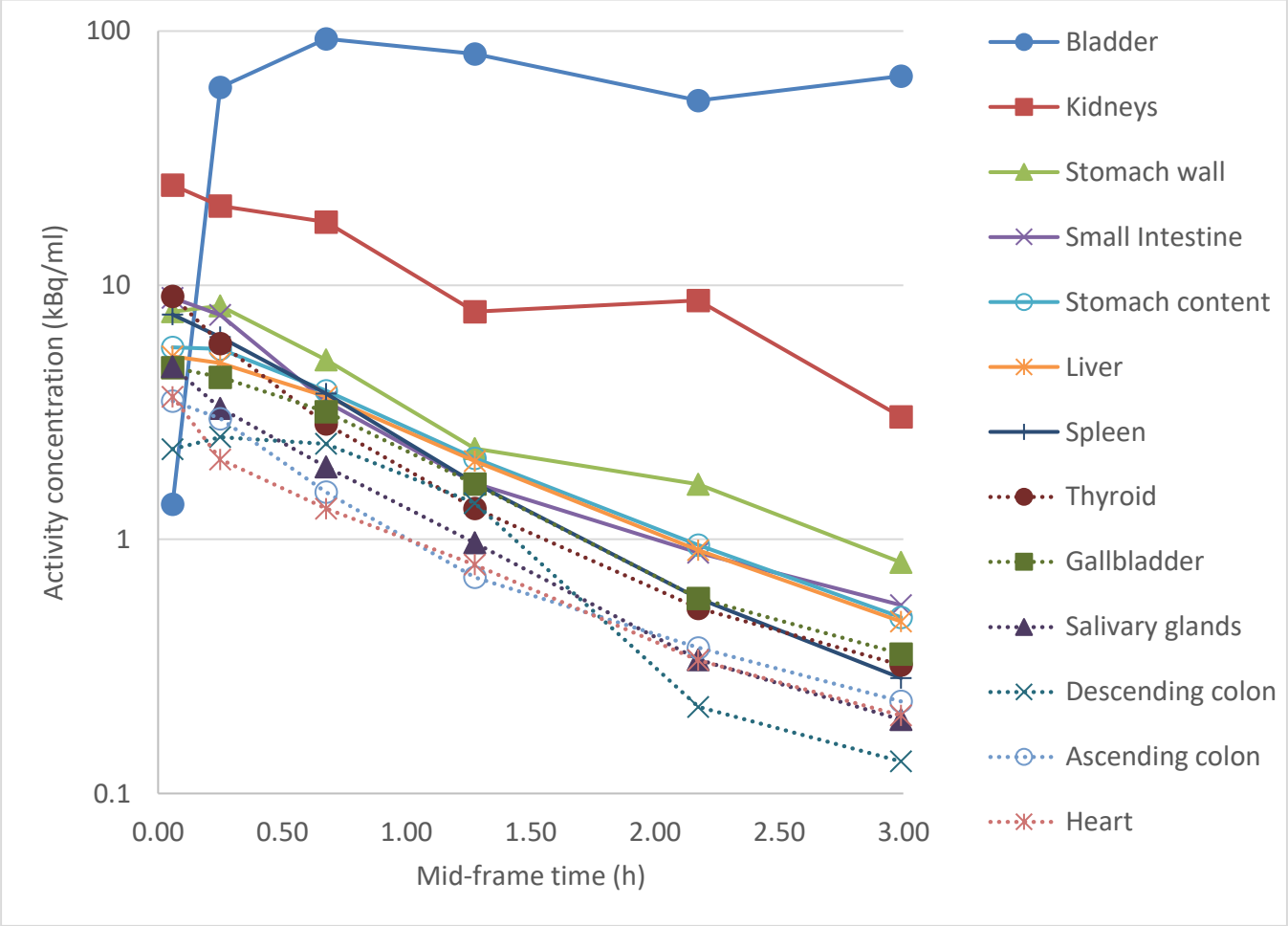

# References


Annes, J.P., D.B. Rifkin, and J.S. Munger. 2002. 'The integrin (alpha)V(beta)6 binds and activates latent TGF(beta)3', *FEBS Letters*, 511: 65-68.

Bates, R. C., D. I. Bellovin, C. Brown, E. Maynard, B. Wu, H. Kawakatsu, D. Sheppard, P. Oettgen, and A. M. Mercurio. 2005. 'Transcriptional activation of integrin β6 during the epithelial-mesenchymal transition defines a novel prognostic indicator of aggressive colon carcinoma', *Journal of Clinical Investigation*, 115: 339-47.

Breuss, J. M., J. Gallo, H. M. DeLisser, I. V. Klimanskaya, H. G. Folkesson, J. F. Pittet, S. L. Nishimura, K. Aldape, D. V. Landers, W. Carpenter, N. Gillett, D. Sheppard, M. A. Matthay, S. M. Albelda, R. H. Kramer, and R. Pytela. 1995. 'Expression of the β6 integrin subunit in development, neoplasia and tissue repair suggests a role in epithelial remodeling', *Journal of Cell Science*, 108: 2241-51.

Burman, A., S. Clark, N. G. A. Abrescia, E. E. Fry, D. I. Stuart, and T. Jackson. 2006. 'Specificity of the VP1 GH loop of foot-and-mouth disease virus for αv integrins', *Journal of Virology*, 80: 9798-810.

Busk, M., R. Pytela, and D. Sheppard. 1992. 'Characterization of the integrin αvβ6 as a fibronectin-binding protein', *Journal of Biological Chemistry*, 267: 5790-96.

Hausner, S.H., D. DiCara, J. Marik, J.F. Marshall, and J.L. Sutcliffe. 2007. 'Use of a peptide derived from foot-and-mouth disease virus for the noninvasive imaging of human cancer: Generation and evaluation of 4-[ 18F]fluorobenzoyl A20FMDV2 for in vivo imaging of integrin (alpha)v(beta)6 expression with positron emission tomography', *Cancer Research*, 67: 7833-40.

Hausner, S.H., D.L. Kukis, M.K. Gagnon, C.E. Stanecki, R. Ferdani, J.F. Marshall, C.J. Anderson, and J.L. Sutcliffe. 2009. 'Evaluation of [64Cu]Cu-DOTA and [64Cu]Cu-CB-TE2A chelates for targeted positron emission tomography with an alphavbeta6-specific peptide', *Molecular imaging : official journal of the Society for Molecular Imaging*, 8: 111-21.

Hays, Marguerite T, Evelyn E Watson, Stephen R Thomas, and Michael Stabin. 2002. 'MIRD dose estimate report no. 19: radiation absorbed dose estimates from 18F-FDG', *Journal of Nuclear Medicine*, 43: 210-14.

Henderson, N.C., and D. Sheppard. 2013. 'Integrin-mediated regulation of TGF+¦ in fibrosis', *Biochimica et Biophysica Acta - Molecular Basis of Disease*, 1832: 891-96.

Hussain, M., K. Miller, I. Rybicka, and R. Bruns. 2014. 'Primary outcomes of the placebo-controlled phase 2 study PERSEUS (NCT01360840) investigating two dose regimens of abituzumab (DI17E6, EMD 525797) in the treatment of chemotherapy-naive patients (pts) with asymptomatic or mildly symptomatic metastatic castration-resistant prostate cancer (mCRPC)', *Journal of Clinical Oncology*, 32.

Jackson, T., D. Sheppard, M. Denyer, W. Blakemore, and A. M. Q. King. 2000. 'The epithelial integrin αvβ6 is a receptor for foot-and-mouth disease virus', *Journal of Virology*, 74: 4949-56.

Janes, S. M., and F. M. Watt. 2006. 'New roles for integrins in squamous-cell carcinoma', *Nature Reviews Cancer*, 6: 175-83.

John, A.E., J.C. Luckett, A.L. Tatler, R.O. Awais, A. Desai, A. Habgood, S. Ludbrook, A.D. Blanchard, A.C. Perkins, R.G. Jenkins, and J.F. Marshall. 2013. 'Preclinical SPECT/CT imaging of (alpha)v(beta)6 integrins for molecular stratification of idiopathic pulmonary fibrosis', *Journal of Nuclear Medicine*, 54: 2146-52.

Kawashima, A., S. Tsugawa, A. Boku, M. Kobayashi, T. Minamoto, I. Nakanishi, and Y. Oda. 2003. 'Expression of αv integrin family in gastric carcinomas: Increased αvβ6 is associated with lymph node metastasis', *Pathology Research and Practice*, 199: 57-64.

Kraft, S., B. Diefenbach, R. Mehta, A. Jonczyk, G. A. Luckenbach, and S. L. Goodman. 1999. 'Definition of an unexpected ligand recognition motif for αvβ6 integrin', *Journal of Biological Chemistry*, 274: 1979-85.

Monaghan, P., S. Gold, J. Simpson, Z. Zhang, P. H. Weinreb, S. M. Violette, S. Alexandersen, and T. Jackson. 2005. 'The αvβ6 integrin receptor for Foot-and-mouth disease virus is expressed constitutively on the epithelial cells targeted in cattle', *Journal of General Virology*, 86: 2769-80.

Munger, J.S., X. Huang, H. Kawakatsu, M.J.D. Griffiths, S.L. Dalton, J. Wu, J.F. Pittet, N. Kaminski, C. Garat, M.A. Matthay, D.B. Rifkin, and D. Sheppard. 1999. 'The integrin (alpha)v(beta)6 binds and activates latent TGF(beta)1: A mechanism for regulating pulmonary inflammation and fibrosis', *Cell*, 96: 319-28.

Nystrom, M. L., D. McCulloch, P. H. Weinreb, S. M. Violette, P. M. Speight, J. F. Marshall, I. R. Hart, and G. J. Thomas. 2006. 'Cyclooxygenase-2 inhibition suppresses αvβ 6 integrin-dependent oral squamous carcinoma invasion', *Cancer Research*, 66: 10833-42.

Onega, Mayca. 2017. 'Preclinical evaluation of [18F]IMAFIB as a selective marker for αVβ6 integrin using positron emission tomography in vivo', *TBD*, in progress.

Popov, Yury, Eleonora Patsenker, Felix Stickel, Jessica Zaks, K. Ramakrishnan Bhaskar, Gerald Niedobitek, Armin Kolb, Helmut Friess, and Detlef Schuppan. 2008. 'Integrin αvβ6 is a marker of the progression of biliary and portal liver fibrosis and a novel target for antifibrotic therapies', *Journal of Hepatology*, 48: 453-64.

Prieto, A. L., G. M. Edelman, and K. L. Crossin. 1993. 'Multiple integrins mediate cell attachment to cytotactin/tenascin', *Proceedings of the National Academy of Sciences of the United States of America*, 90: 10154-58.

Roberts, A. B., and M. B. Sporn. 1989. 'Regulation of endothelial cell growth, architecture, and matrix synthesis by TGF-β', *American Review of Respiratory Disease*, 140: 1126-28.

Roberts, A. B., M. B. Sporn, and R. K. Assoian. 1986. 'Transforming growth factor type β: Rapid induction of fibrosis and angiogenesis in vivo and stimulation of collagen formation in vitro', *Proceedings of the National Academy of Sciences of the United States of America*, 83: 4167-71.

Saha, A., D. Ellison, G. J. Thomas, S. Vallath, S. J. Mather, I. R. Hart, and J. F. Marshall. 2010. 'High-resolution in vivo imaging of breast cancer by targeting the pro-invasive integrin alphavbeta6', *J Pathol*, 222: 52-63.

Saini, Gauri, Joanne Porte, Paul H. Weinreb, Shelia M. Violette, William A. Wallace, Tricia M. McKeever, and Gisli Jenkins. 2015. 'αvβ6 integrin may be a potential prognostic biomarker in interstitial lung disease', *European Respiratory Journal*.

Slack, Robert J, Maryam Hafeji, Rebecca Rogers, Steve B Ludbrook, John F Marshall, David J Flint, Susan Pyne, and Jane C Denyer. 2016. 'Pharmacological Characterization of the αvβ6 Integrin Binding and Internalization Kinetics of the Foot-and-Mouth Disease Virus Derived Peptide A20FMDV2', *Pharmacology*, 97: 114-25.

Stabin, Michael G, and Jeffry A Siegel. 2003. 'Physical models and dose factors for use in internal dose assessment', *Health physics*, 85: 294-310.

Stabin, Michael G, Richard B Sparks, and Eric Crowe. 2005. 'OLINDA/EXM: the second-generation personal computer software for internal dose assessment in nuclear medicine', *Journal of Nuclear Medicine*, 46: 1023-27.

Thomas, B. J., O. K. Kan, K. L. Loveland, J. A. Elias, and P. G. Bardin. 2016. 'In the shadow of fibrosis: Innate immune suppression mediated by transforming growth factor-β', *American Journal of Respiratory Cell and Molecular Biology*, 55: 759-66.

Thomas, G. J., I. R. Hart, P. M. Speight, and J. F. Marshall. 2002. 'Binding of TGF-β1 latency-associated peptide (LAP) to αvβ6 integrin modulates behaviour of squamous carcinoma cells', *British Journal of Cancer*, 87: 859-67.

Thomas, G.J., M.P. Lewis, I.R. Hart, J.F. Marshall, and P.M. Speight. 2001. '(alpha)V(beta)6 integrin promotes invasion of squamous carcinoma cells through up-regulation of matrix metalloproteinase-9', *International Journal of Cancer*, 92: 641-50.

Thomas, G.J., M.L. Nystrom, and J.F. Marshall. 2006. '(alpha)v(beta)6 integrin in wound healing and cancer of the oral cavity', *Journal of Oral Pathology and Medicine*, 35: 1-10.